Power losses analysis of multiphase DC-DC buck converter using OrCAD PSpice software

Ahmad Faiz Hilmi Abdul Ghani, Mhd Hazwaj Poad, Afarulrazi Abu Bakar, Siti Nuraini Norazman, Mohd Azlee Noor Amran
Faculty of Electrical and Electronic Engineering, University Tun Hussein Onn Malaysia, Johor, Malaysia

ABSTRACT

DC-DC buck converters have wide applications in portable electronic devices, battery chargers, and telecommunications. However, single-phase DC-DC buck converters have some drawbacks, especially in high current applications, where the increase in the size of the inductor will increase power losses, which significantly affects the overall efficiency of the converter. The multiphase configuration offers several advantages, such as reduction in output voltage ripple, input current ripple, conduction loss, and the physical size of the hardware. This paper presents an analysis of the power losses of the multiphase DC-DC buck converter with output power ranging between 50 watts to 250 watts. To verify the effectiveness of the multiphase converter, performance analysis was done using OrCAD PSpice software, where the number of phases was limited to five phases. This paper focused on power losses in the converter, namely conduction losses in diodes and MOSFETs, switching loss in MOSFETs, as well as losses in the inductor and capacitor. The relationship between the number of phases and factors of switching frequency, output, and the components' internal resistance was also highlighted and discussed in detail.

Corresponding Author:

Mhd Hazwaj Poad
Faculty of Electrical and Electronic Engineering, University Tun Hussein Onn Malaysia
Parit Raja, Batu Pahat, Johor, Malaysia
Email: hazwaj@uthm.edu.my

1. INTRODUCTION

Nowadays, DC-DC converters play an essential role in stabilizing output voltage and have received an overwhelming demand in many applications, such as PV systems [1], portable computers [2], mobile phones, electric vehicles (EV) [3], telecommunication power systems [4], and grid-connected systems [5]. A buck converter is a step-down DC-DC converter where the DC output voltage is lower than the DC input voltage. The buck converter is from the family of switched-mode power supply (SMPS) that contains at least two semiconductors, which are a diode and a transistor, and at least one energy storage, which is a capacitor, an inductor, or both. Thus, it is widely used in many applications, for instance, in advanced telecom and datacom systems, as the interface between the battery and the components in portable computers, and as a point-of-load (POL) converter in servers. Theoretically, power dissipation and efficiency start to exhibit problems in high current, which cause all power output to flow through the inductor, and the switch in a single converter may cause high conduction power loss. To overcome these problems, a multiphase configuration can be used, as it can significantly reduce the ripple current at the input and output converters [6]–[8]. In addition, it can reduce conduction loss at each switch by spreading the current to all phases [9].

The multiphase buck regulator is a set of multiple single buck converters connected in parallel [10], where every phase has its individual inductor and power switches. As a result, current is spread out equally within the switching cycle, and output current and voltage ripples decrease as the number of phase increases. Therefore, it has been used in many cooling applications because the power conversion works efficiently to reduce heat and extend the battery's lifespan.

There are several advantages of using the multiphase buck converter compared with using the conventional buck converter, such as reduced input and output ripple currents, improved thermal performance, and high efficiency [6]. Also, the phases are shared by both input and output capacitors in the circuit design to reduce ripples and to store and supply electrical energy. Therefore, the interleaving PWM switching signal employed with the multiphase buck converter is the best solution to deliver electrical supply to any microprocessor that requires high current with lower input and output current ripples. Moreover, the converter can operate with a high switching frequency of input and output capacitors compared with the single buck converter. Even though this will raise switching loss, it can make the converter operate at a high frequency, which is better in terms of output voltage ripple than using the single buck converter [11]. In addition, the maximum reduction of instantaneous input current causes low ripple noise to flow back into the power supply [12]. The low value of the capacitor is sufficient to eliminate ripples and reduce the variation in current. Apart from the advantages as mentioned earlier, researchers have come with various research on multiphase related to current balancing [13], [14], soft-switching [9], coupled inductor [15]–[17], ripple minimization [18] and robust controlled [19], [20].

This paper presents the analysis of a multiphase DC-DC buck converter with the interleaving switching signal. It focused on the power losses analysis of the multiphase DC-DC buck converter, which were the total inductor loss, capacitor loss, switching loss (FETs), and conduction loss (FETs and diodes). The analysis was performed from 1 phase up to 5 phases with output power of 50 W, 100 W, 150 W, 200 W, and 250 W. In detail, this paper provides an overview and projection for design guidelines in a multiphase DC-DC buck converter regarding the losses occurring concerning the number of phases. The results were compared and analyzed in terms of duty cycle and the number of phases. Finally, the efficiency and performance of the multiphase boost converters were compared.

2.   MULTIPHASE BUCK CONVERTER'S TOPOLOGY

In general, DC-DC converters can be designed to operate either in continuous conduction mode (CCM) or discontinuous conduction mode (DCM). The mode of operation depends on the value of resistance load, the size of storage elements, and the switching frequency of the system. In CCM, the output regulation has lower inductor current ripple. On the other hand, the operation of the DCM has advantages, such as faster transient response, reduced diode reverse recovery loss, and also reduced electromagnetic interference (EMI) [21]. The difference between DCM and CCM is that the current of the inductor during energy transfer in DCM falls to zero levels, but in CCM, it does not.

Figure 1 shows the circuit diagram of the 5-phase buck converter, which is also known as the step-down converter and Figure 2 shows the 5-phase inductor current with interleaving. The components used in this converter are quite similar to those in a boost converter, but the placement of the inductor and the semiconductor switch are different. The inductor in the converter charges and stores electrical energy when the switch is closed, and discharges when the switch is opened, to maintain a continuous supply to the load. Figure 3 shows the waveforms of inductor current ripple and switching pulse at output power of 50 W for the 1-phase buck converter with duty cycle of 0.15.

The topology of the multiphase buck converter consists of several conventional buck converters connected in parallel, and all share the typical load. Each phase uses a single inductor, but the phases share the same output capacitor. The interleaving switching operation can significantly reduce inductor current at each stage. In addition, inductor constraint can be reduced, where high ripple current that flows through the inductor will cancel each other partially at the output.

The normalized ripple current, $I_{RippleN}$, in a multiphase buck converter can be determined as in (1) [22]:

$$I_{RippleN} = N_{phase} \times \frac{\left[D - \frac{m}{N_{phase}}\right] \times \left[\frac{1+m}{N_{phase}} - D\right]}{(1-D) \times D} \tag{1}$$

where D is duty cycle and N_{phase} is the number of phases, while m is known as the floor, which can be obtained by using (2):

$$m = D \times N_{phase} \tag{2}$$

In (2) is used to determine the number of phases depending on the required ripple current. This shows that the percentage of ripple current cancelled in each inductor. The normalized root mean square (RMS) input current capacitance of regulator, $I_{CInputN}$, can be calculated by using (3):

$$I_{CInputN} = \sqrt{\left[D - \frac{m}{N_{phase}} \right] \times \left[\frac{1+m}{N_{phase}} - D \right] m} \tag{3}$$

The normalized ripple current of output capacitance, $I_{COutputN}$, is calculated by using (4):

$$I_{COutputN} = \frac{N_{phase}}{D \times (1-D)} \times \left(D - \frac{m}{N_{phase}} \right) \times \left(\frac{1+m}{N_{phase}} - D \right) \tag{4}$$

The switches are connected in parallel. Active switches suffer from input voltage, and thus only devices with rated voltage higher than input voltage can be applied. PWM signal with a fixed frequency is commonly used to regulate output voltage. In one period, the signal will be on and off. Output voltage is related to input voltage and can be determined using (5):
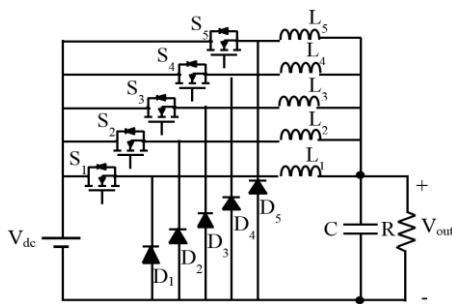
$$V_{out} = D \times V_{in} \tag{5}$$

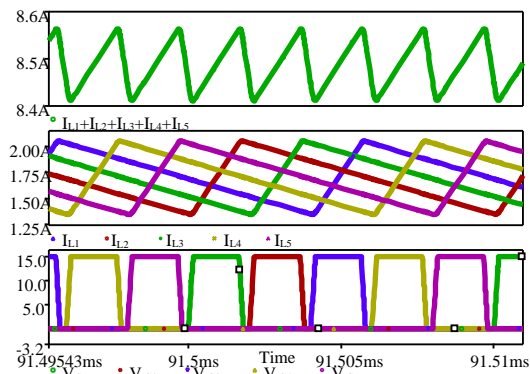Figure 1. 5-phase buck converter's configuration

Figure 2. 5-phase inductor current with interleaving switching signals

Figure 3 shows the normalized RMS input capacitance current versus the regulator's duty cycle for different number of phases. Based on Figure 3, the addition of phases may reduce more than half 50% of RMS current at a particular duty cycle.
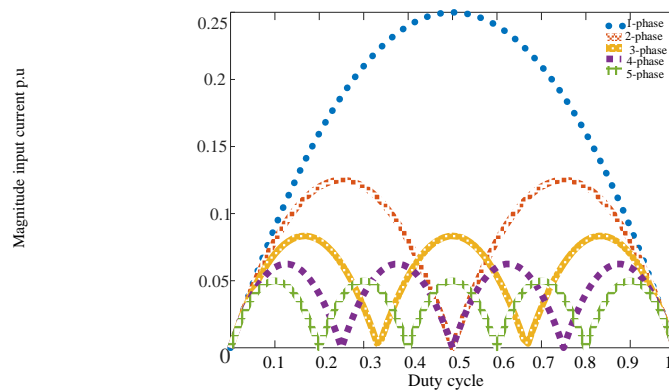

Figure 3. Concept of input current ripple with variation in the number of phases

3. CURRENT RIPPLE

Based on the rule of thumb, inductor current ripple is designed to be almost 30% of average inductor current. The theoretical derivation of the ratio of ripple current over average current is known as the ripple factor, which is a method to obtain suitable inductor size [23]. The arrangement of the inductor and capacitor provides effective filtering of inductor current ripple. In addition, the buck converter and its derivatives have deficient characteristics of output ripple. Therefore, this converter is typically operated in CCM, where the peak inductor current is low, requiring a small smoothing capacitor [24].

Peak inductor current ripple is the maximum current that the inductor can store before being saturated. Saturated means that transistor switching continues to turn on for a longer time even when the inductor exceeds the maximum current storage capacity. This is an unwanted situation, which needs to be avoided. The minimum inductor current is the minimum current that can be allowed by the inductor during the discharging of its stored energy in the form of back electromotive force (EMF). This is when the transistor turns off and the inductor's stored current drops drastically towards zero. Before the current reaches zero, the transistor must turn on again, and the current at this point is called the minimum inductor current [25]. However, if the transistor continues to turn off and inductor current reaches zero, this situation is known as the discontinuous mode.

Ripple current is the difference between peak current and the minimum current induced in the buck converter. Therefore, the capacitor is used as a filter to stabilize the ripple current and make it almost constant. The suitability of output capacitance is very important for a low-noise design. Hence, the correct capacitor will deliver low cost, low equivalent series resistance (ESR), and high capacitance [26].

4. POWER LOSSES

Several losses should be carefully considered, which are conduction loss, switching loss, inductor loss, and capacitor loss. Therefore, the total power losses in a converter are as shown in (6):

$$P_{total} = P_{cond} + P_{SW-H} + P_L + P_{CAP} \tag{6}$$

4.1 Conduction loss

Conduction loss occurs at the high-side MOSFET, P_{on-H}, which is determined by on-resistance, output current, and on-duty-cycle. The loss occurs when the switch is on while the diode is reverse-biased. In this research, the R_{on-H} value was obtained from the datasheet of the selected N-channel power MOSFET, which was IRF1404. Thus, the loss is calculated by using (7):

$$P_{on\text{-}H} = I_{out^2} \times R_{on} - H \times \frac{V_{out}}{V_{in}} \tag{7}$$

Conduction loss in MOSFETs for a DC-DC buck converter can be divided into two, which are for the high-side MOSFET (HMOS) and the low-side MOSFET (LMOS). Conduction loss is caused by the on-resistance of the low-side MOSFET. Conduction losses P_{on-H} and P_{on-L} for the buck converter are calculated by using (8) and (9):

$$P_{Non\text{-}H} = I_{out}^2 \times R_{on-H} \times \frac{V_{out}}{V_{in}} \tag{8}$$

$$P_{on\text{-}L} = I_{out}^2 \times R_{on-L} \times \left(1 - \frac{V_{out}}{V_{in}} \right) \tag{9}$$

On the other hand, conduction loss in diodes occurs during the forward voltage (V_F) condition because the diode acts as a short circuit, and its value will tend to be more significant compared with those of the MOSFETs. During reverse bias, the diode acts as an open circuit because there is no dissipated power due to no current flowing through it. Therefore, if the high-side MOSFET is switched off, the loss in the diode can be calculated by using (10):

$$P_{COND\text{-}D} = V_F \times I_{out} \times \left(1 - \frac{V_{out}}{V_{in}} \right) \tag{10}$$

4.2 Switching loss

A simple geometric equation can be used to calculate the switching loss in MOSFETs. Switching loss is similar to conduction loss, in that it consists of two types of switching losses, which are losses in the HMOS and LMOS [27]. The switching loss in the HMOS, P_{SW-H}, is calculated as in (11):

$$P_{SW\text{-}H} = \frac{1}{2} \times V_{in} \times I_{out} \times \left(T_{r-H} + T_{f-H}\right) \times f_{sw} \tag{11}$$

Switching loss in the LMOS occurs when the gate voltage turns on the LMOS, and at the same time, the body of the diode is energized. Then, the FET is turned off by the gate voltage, and load current continues to flow through the body of the diode in the same direction. Drain voltage and forward-direction voltage will become the same and are still low. As a result, the switching loss at the LMOS becomes minimal and can be calculated as in (12) [27]:

$$P_{SW\text{-}L} = \frac{1}{2} \times V_D \times I_{out} \times \left(T_{r-L} + T_{f-L}\right) \times f_{sw} \tag{12}$$

4.3 Inductor loss

This research only focused on conduction loss in the inductor. The DC resistance (DCR) of the winding is used to form the inductor, producing conduction loss. DCR increases as wire length increases, but this can cause the cross-section of the wire to increase. Also, when DCR increases, the value of inductance increases. When DCR decreases, inductor's case size increases [27]. Conduction loss in an inductor, P_L, can be calculated by using (13) [28]:

$$P_L = I_{out}^2 \times R_{DCR} \tag{13}$$

4.4 Capacitor loss

There are some losses within the capacitor, which are series resistance, leakage, and dielectric losses. These losses are simplified as the equivalent series resistance (ESR) loss. Hence, all of the losses can be calculated by multiplying the square of the RMS current of a capacitor with the equivalent series resistance of the capacitor [27]. Power losses that occur in the capacitor are calculated by multiplying R_{ESR} with the RMS AC current that flows through the capacitor. However, the RMS current in the output capacitor should be determined in advance to calculate the losses in the capacitor. The RMS current in the output capacitor is equal to the ripple current in the inductor and can be calculated as in (14):

$$I_{COUT(RMS)} = \frac{\Delta I_{L(AVG)}}{2\sqrt{3}} \tag{14}$$

To maintain an acceptable current ripple and output voltage ripple at the inductor, the switching frequency should be reduced. Capacitor loss can be calculated by using (15):

$$P_{CAP} = I_{CAP(RMS)}^2 \times R_{ESR} \tag{15}$$

5 CIRCUIT SIMULATION

Table 1 shows the specifications of the parameters used in designing the multiphase DC-DC buck converter's circuit. The components in the simulation software were set according to the parameters' values. The phases were set from 1 up to 5 phases and switching frequency was set to 100 kHz, with output power of 50 W, 100 W, 150 W, 200 W, and 250 W.

Table 1. Components' parameter values

Parameter	Value
Input voltage, V_{in}	12 V
Inductance, $L_1 = L_2 = L_3 = L_4 = L_5$	22 μH
Capacitance, C	470 μF

To ensure that inductor current was always in CCM, the value of the inductor must be higher than the minimum value. To obtain the minimum value of the output capacitor, inductor current ripple must be identified in advance by using the recommended inductor value. Furthermore, output voltage ripple should

also be acquired before calculating the minimum capacitor value. The estimation for inductor current ripple is shown in (16), while the estimation for the output voltage ripple is shown in (17):

$$\Delta I_L = \frac{(V_{in} - V_{out}) \times D}{f_{sw} \times L} \tag{16}$$

$$C_{min} = \frac{\Delta I_L}{8 \times f_{sw} \times \Delta V_{out}} \tag{17}$$

The voltage pulse connected to each MOSFET functions as the PWM generator to trigger the MOSFETs (on and off). Time delay (T_D) can be calculated using (18), which subsequently results in continuous interleaved switching pulses.

$$T_D = \frac{1}{N - phase} \tag{18}$$

To calculate inductor and capacitor losses, the average inductor current ripple must be calculated in advance, as shown in (19):

$$\Delta I_{L(avg)=} \frac{I_{max} + I_{min}}{2} \tag{19}$$

To reduce ripple at the output current, a large capacitor is required. Output ripple current factor can be obtained by using (20):

$$\Delta I_{(FACTOR)} = \frac{I_{max} - I_{min}}{I_{avg}} \tag{20}$$

6   INPUT CURRENT RIPPLE'S PERFORMANCE

The outputs of voltage, current, and power were taken by adjusting the values of resistance and duty cycle to ensure the circuit was in CCM. The analysis of the multiphase buck converters was based on the effects of output current ripple and inductor current ripple to calculate conduction loss, switching loss, inductor loss, and capacitor loss by using OrCAD PSpice software. Based on the overall results in this section, the higher the number of phases, the lower were the ripple output current and inductor current in the buck converter design. In addition, output current and output voltage indicated reduced ripples on the respective waveforms. The duty cycle was selected depending on the minimum inductor current ripple because each inductor only can withstand not more than 15 A. Therefore, the lowest average inductor current ripples were chosen, which are shown in Figure 4. There were a few inductors current ripples that exceeded the limit of the rated inductor current, which occurred in the 1-phase and 2-phase buck converters. This shows that the circuit would become a short circuit if an experiment were conducted on their hardware.

The 1-phase buck converter started to produce high peak current at output power of 100 W, which continued to increase drastically until 250 W. The 2-phase buck converter showed a significant reduction in the average value of inductor current ripple compared with the 1-phase converter. However, at high output power, it still exceeded the inductor current limit. In this case, it gave more stress to the MOSFETs and may cause discontinuous design operation.

The duty cycles for the 1-phase converter until the 5-phase converter were almost similar because of the considerable difference in duty cycle's effect on output voltage and current, as well as on inductor current ripple. This means that the chosen duty cycles did not cause inductor current to reach zero and the converters to operate in discontinuous mode. Therefore, the selection of duty cycle was essential to ensure that the multiphase buck converters continuously operated in CCM.

To obtain the desired output power, the resistor was adjusted to increase and decrease the output load. The relationship between the value of the resistor and output power was that the lower the value of the resistor, the higher was the output power produced. The results show that the output current increased, while the output voltage decreased, with reduced resistance. The output voltage results did not reach the output voltage's calculated value, which means that the design was in continuous mode and the MOSFETs were switched on. If the simulated output voltage reached the predetermined voltage, it would cause the system to operate in DCM.
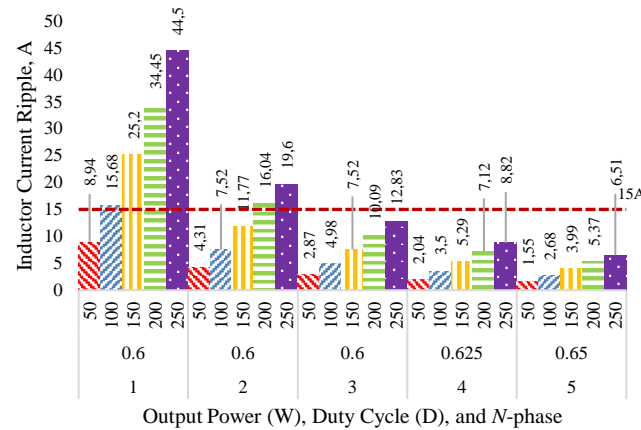
Figure 4. Graph of inductor current ripple against output power, selected duty cycle, and *N*-phase

7   POWER LOSSES ANALYSIS

This section focuses only on four types of losses: conduction loss at the MOSFETs and diodes, switching loss at MOSFETs, inductor loss, and capacitor loss. These losses were derived from the formulas shown in section 4.

7.1. Conduction loss

Conduction losses for each MOSFET and diode were calculated using (7) and (10). All values of output currents and output voltages were measured from simulation, while R_{on-H} for the MOSFETs was obtained from the datasheet provided by the manufacturer. R_{on-H} and V_F of the power diode were 0.004 Ω and 0.41 V, respectively. Table 2 shows that the diodes contributed a higher loss compared with the MOSFETs.

Based on Table 2, the increase in the number of phases led to the reduction in losses in the MOSFET and diode components. These losses involved both components in each phase. Consequently, the losses displayed a substantial rise in each increased phase. Figure 5 shows the conduction loss graph for the 1-phase to 5-phase buck converters against the selected duty cycles and output power.

Table 2. Conduction loss in MOSFETs and diodes

| Number of Phases	Duty Cycle (D)	Output Power (W)	Conduction Loss (W)		Total Conduction Losses (W)
			MOSFETs	Diodes	
1	0.6	50	0.18	1.62	1.80
		100	0.53	2.98	3.51
		150	1.28	5.12	6.40
		200	2.32	7.22	9.54
		250	3.82	9.44	13.27
2	0.6	50	0.17	1.50	3.35
		100	0.51	2.69	6.39
		150	1.21	4.36	11.14
		200	2.20	6.12	16.63
		250	3.21	7.67	21.75
3	0.6	50	0.17	1.48	4.96
		100	0.51	2.62	9.39
		150	1.14	4.03	15.53
		200	2.03	5.53	22.66
		250	3.23	7.18	31.22
4	0.625	50	0.16	1.30	5.85
		100	0.47	2.26	10.93
		150	1.07	3.48	18.19
		200	1.92	4.76	26.70
		250	2.92	5.96	35.51
5	0.65	50	0.15	1.15	6.50
		100	0.45	2.00	12.27
		150	1.00	3.02	20.08
		200	1.81	4.11	29.58
		250	2.87	5.25	40.59
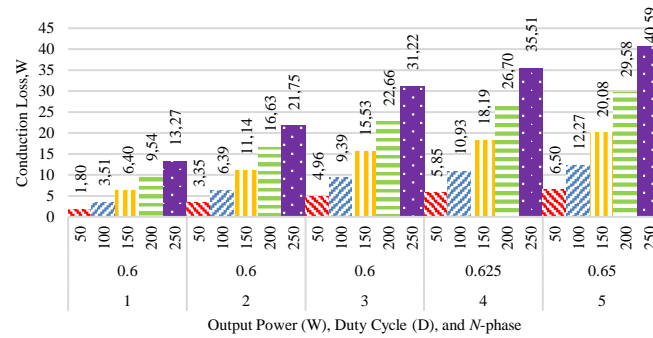
Figure 5. Graph of total conduction losses (MOSFETs and diodes) against output power, duty cycle, and *N*-phase

7.2. Switching loss

Switching losses were calculated for each MOSFET switch at every phase of the multiphase buck converter. The losses were calculated by using the formulas in (11) and (12). Rising time (T_r) and falling time (T_f) were measured from the waveforms at one level only, which means that, to represent the switching times at other levels, the losses were multiplied by the number of phases. Figure 6 shows the switching loss graph for the 1-phase to 5-phase buck converters against the selected duty cycles and output power.

Figure 6 clearly shows that switching loss increased with increasing output power when the number of phases increased. This is because switching loss is proportional to the total number of phases. After all, as the number of phases of the buck converter increases, the number of MOSFETs used also increases. The loss considers the switching loss in the MOSFETs in each phase, which is the same concept used for conduction loss. Thus, the loss was not too high compared with the conduction loss.
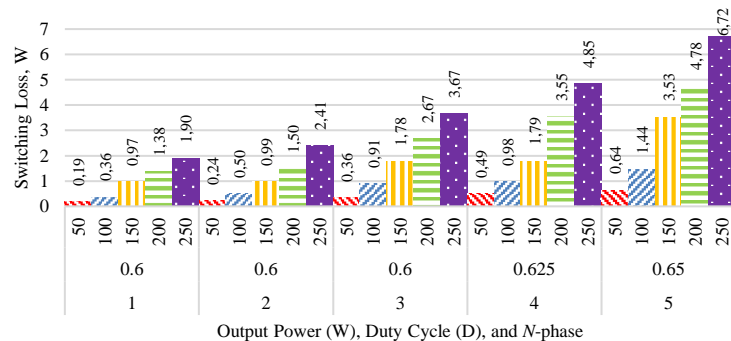
Figure 6. Graph of switching loss against output power, duty cycle, and *N*-phase

7.3. Inductor loss

Inductor loss can be determined by using (13). Since an inductor is always energized either during on-state or off-state, this means that it is not affected by duty cycle. In addition, the loss in an inductor is proportional to the square of the average inductor current, which produces higher output current and results in an increased loss for each inductor component. Therefore, it is crucial to choose a suitable inductor. R_{DCR} was obtained from the spreadsheet of the 22 µH inductor, which was 30 mΩ. The higher the R_{DCR}, the higher is the increase in inductor loss. Figure 7 shows the inductor loss graph for the 1-phase to 5-phase buck converters against the selected duty cycles.

Figure 7 shows that inductor loss decreased as the number of phases increased and output power increased. Extreme reductions are observed in the 1-phase and 2-phase converters, especially for output power of 150 W, 200 W, and 250 W. Although the loss in the inductor considered the losses for all inductor components, the loss that occurred in the 1-phase converter was more significant than in the other converters. Based on the overall inductor loss result for the 2-phase to 5-phase buck converters, most losses were below

20 W, except for output power of 250 W for the 2-phase converter. This indicated that the inductor operated efficiently in each increased phase.
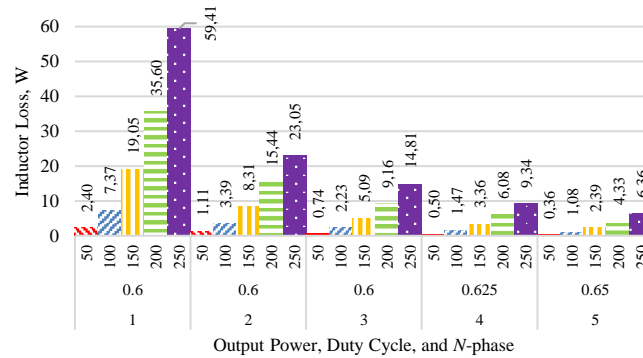

Figure 7. Graph of inductor loss against output power, duty cycle, and *N*-phase

7.4. Capacitor loss

Capacitor loss was determined using (15). R_{ESR} was obtained from the spreadsheet of the 470μF capacitor, which was 29 mΩ. The higher the R_{ESR}, the more losses would occur in the capacitor component. Figure 8 shows the capacitor loss graph for the 1-phase to 5-phase buck converters against selected duty cycles and output power of 50 W, 100 W, 150 W, 200 W, and 250 W.

Capacitor loss decreased as the number of phases increased and output power increased. Maximum loss occurred in the 1-phase buck converter, and minimum loss occurred in the 5-phase buck converter. The graph shows a massive loss reduction between the 1-phase and 2-phase converters, particularly for output power of 150 W, 200 W, and 250 W. Output power of 50 W resulted in power loss of fewer than 1 W except in the 1-phase buck converter. This indicated that the capacitor operated efficiently in each increased phase.
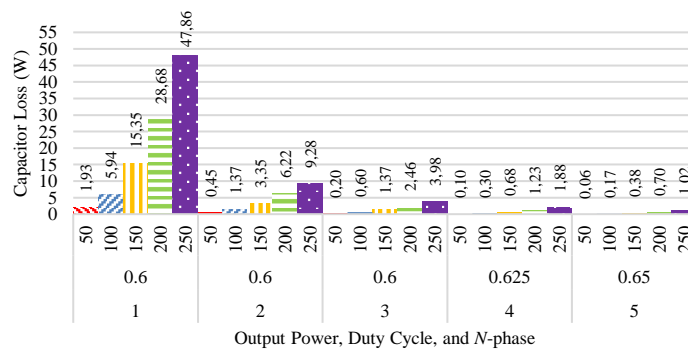
Figure 8. Graph of capacitor loss against output power, duty cycle, and *N*-phase

7.5. Overall power losses

Conduction, switching, inductor, and capacitor losses were analyzed in detail for each output power of 50 W, 100 W, 150 W, 200 W, and 250 W. Conduction loss and switching loss indicated a constant increase as the number of phases increased. This was because the number of MOSFETs and diodes used increased as the number of phases increased. However, inductor loss and capacitor loss indicated a constant decrease as the number of phases increased. The decline in these losses depended on the average inductor current, R_{DCR}, and R_{ESR}. The lower the R_{DCR} and R_{ESR}, the higher the power loss reduction was for both components.

Figure 9 shows that the 1-phase of buck converter had the largest power loss, while the other converters had relatively small losses and small loss differences. This shows that adding a new phase into the buck converter can reduce the power loss for each component. In addition, the most significant conduction loss occurred in the 2-phase to 5-phase buck converters. Switching loss showed a slight increase but still

mostly below 2 W at various number of phases and output power values. Although switching loss and conduction loss increased with increasing number of phases, inductor and capacitor losses showed the opposite result and were significantly lower for the 1-phase and 2-phase converters. Power losses in the capacitor were all less than inductor losses for all number of phases.

As shown in Figure 10, efficiency decreased slightly as output power increased. The 2-phase to 5-phase converters can still be considered as well-performing converters, as their overall efficiency exceeded 80%. At 50 W and 100 W, the 2-phase buck converter performed better than the other converters, but it started to have a similar performance as the other converters with further increases in output power. All converters except the 1-phase buck converter showed a similar efficiency of 84% at output power of 200 W. At the highest output power, the efficiency of the 4-phase buck converter was marginally higher than those of the other converters.

The 1-phase buck converter showed an extreme reduction in efficiency at output power from 100 W until 250 W. It began to produce a poor performance at 150 W of output power, which was less than 80%. Nevertheless, it showed excellent performance at light load, which was a similar efficiency performance as that of the 4-phase buck converter. Therefore, from the overall efficiency analysis, it can be concluded that the buck converter is more efficient at light loads and less efficient at high power loads. Also, for a wide range of loads, a high number of phases can be considered, where the deterioration in efficiency is insignificant. Lastly, the increase in the number of phases can help overcome the limitations of the single buck converter, especially with high loads.
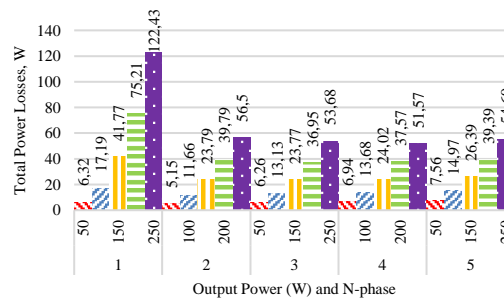

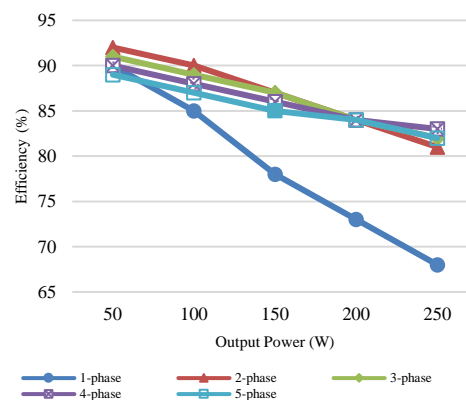Figure 9. Total power losses in 1-phase to 5-phase buck converters

Figure 10. Comparison graph of efficiency of 1-phase to 5-phase buck converters

8 CONCLUSION

In conclusion, 1-phase to 5-phase multiphase buck converters were designed and simulated in OrCAD PSpice software. The results obtained from the simulation were analyzed to determine the conduction loss in MOSFETs and diodes, switching loss in MOSFETs, inductor loss for each inductor component, and capacitor loss at different duty cycles and output power settings based on the number of phases. It has been shown that the 2-phase buck converter was very optimal and more efficient at light loads

(<200 W). Still, power dissipation and efficiency started to decrease at heavy loads (>200 W). The best-optimized design for a heavy load was the 4-phase buck converter. Apart from its excellent operation in heavy loads, it can also be considered efficient for light loads. Switching frequency is the most significant factor that contributes to switching losses. It was found that conduction loss was the highest loss in the multiphase buck converter. Therefore, the solution to overcome this problem is that the diodes need to be replaced with MOSFETs. However, this will definitely increase the cost and the complexity of the hardware. Regardless, a multiphase buck converter requires a lot of components, and the controller can become more complex and complicated. Therefore, it has a high tendency of facing the problem of current imbalance between multiple switching phases.

ACKNOWLEDGEMENTS

REFERENCES

[1] B. Chen, Y. Wang, Y. Tian, and S. Wei, "Current Sharing/Voltage Sharing Control Strategy for Cascaded DC/DC Converter in Photovoltaic DC Collection System," in *2018 International Power Electronics Conference, IPEC-Niigata - ECCE Asia 2018*, 2018, pp. 1397–1402, doi: 10.23919/IPEC.2018.8507822.

[2] W. M. Utomo, A. Bakar, M. Ahmad, T. Taufik, and R. Heriansyah, "Online learning neural network control of buck-boost converter," in *Proceedings - 2011 8th International Conference on Information Technology: New Generations, ITNG 2011*, 2011, no. February 2014, pp. 485–489, doi: 10.1109/ITNG.2011.216.

[3] D. M. Bellur and M. K. Kazimierczuk, "DC-DC converters for electric vehicle applications," in *2007 Electrical Insulation Conference and Electrical Manufacturing Expo, EEIC 2007*, 2007, pp. 286–293, doi: 10.1109/EEIC.2007.4562633.

[4] R. Miftakhutdinov, "Power Saving Solutions in DC / DC Converter for Data and Telecommunication Power System Rais Miftakhutdinov," *2009 Int. Conf. Power Electron. Drive Syst.*, pp. 591–596, 2009, doi: 10.1109/PEDS.2009.5385883.

[5] A. A. Bakar, M. A. N. Amran, S. Salimin, M. K. M. Jamri, and A. F. H. A. Gani, "Modeling of Single-Phase Grid-Connected using MATLAB/Simulink Software," *2019 IEEE Student Conf. Res. Dev. SCOReD 2019*, pp. 69–74, 2019, doi: 10.1109/SCORED.2019.8896226.

[6] A. F. H. A. Gani, A. A. Bakar, A. Ponniran, M. Hussainar, and M. A. N. Amran, "Design and development of PWM switching for 5-level multiphase interleaved DC/DC boost converter," *Indones. J. Electr. Eng. Comput. Sci.*, vol. 17, no. 1, pp. 131–140, 2019, doi: 10.11591/ijeecs.v17.i1.pp131-140.

[7] K. Drobnic *et al.*, "An Output Ripple-Free Fast Charger for Electric Vehicles Based on Grid-Tied Modular Three-Phase Interleaved Converters," *IEEE Trans. Ind. Appl.*, vol. 55, no. 6, pp. 6102–6114, 2019, doi: 10.1109/TIA.2019.2934082.

[8] Y. Tao and S. J. Park, "A novel ripple-reduced DC-DC converter," *J. Power Electron.*, vol. 9, no. 3, pp. 396–402, 2009.

[9] A. A. Bakar, M. U. Wahyu, A. Ponniran, and T. Taufik, "Simulation and analysis of multiphase boost converter with soft-switching for renewable energy application," *Int. J. Power Electron. Drive Syst.*, vol. 8, no. 4, pp. 1894–1902, 2017, doi: 10.11591/ijpeds.v8i4.pp1894-1902.

[10] M. K. Kazimierczuk, "*Pulse-Width Modulated DC-DC Power Converters," John Wiley & Sons*, 2015.

[11] R. Miftakhutdinov, "Optimal design of interleaved synchronous buck converter at high slew-rate load current transients," in *PESC Record - IEEE Annual Power Electronics Specialists Conference*, 2001, vol. 3, pp. 1714–1718, doi: 10.1109/PESC.2001.954366.

[12] "Multiphase Buck Converters | Maxim Integrated." . Available : https://www.maximintegrated.com / en / products / power / switching-regulators / multiphase.html.

[13] Y. S. Roh, Y. J. Moon, J. Park, M. G. Jeong, and C. Yoo, "A multiphase synchronous buck converter with a fully integrated current balancing scheme," *IEEE Trans. Power Electron.*, vol. 30, no. 9, pp. 5159–5169, 2015, doi: 10.1109/TPEL.2014.2368130.

[14] G. Eirea and S. R. Sanders, "Phase Current Unbalance Estimation in Multiphase Buck Converters," in *IEEE Transactions on Power Electronics*, vol. 23, no. 1, pp. 137-143, Jan. 2008, doi: 10.1109/TPEL.2007.911840..

[15] W. Huang and B. Lehman, "Analysis and Verification of Inductor Coupling Effect in Interleaved Multiphase DC-DC Converters," in *IEEE Transactions on Power Electronics*, 2016, vol. 31, no. 7, pp. 5004–5017, doi: 10.1109/TPEL.2015.2479191.

[16] J. P. Lee, H. Cha, D. Shin, K. J. Lee, D. W. Yoo, and J. Y. Yoo, "Analysis and design of coupled inductors for two-phase interleaved dc-dc converters," *J. Power Electron.*, vol. 13, no. 3, pp. 339–348, 2013, doi: 10.6113/JPE.2013.13.3.339.

[17] D. Liang and H. B. Shin, "Coupled inductor design method for 2-phase interleaved boost converters," *J. Power Electron.*, vol. 19, no. 2, pp. 344–352, 2019, doi: 10.6113/JPE.2019.19.2.344.

[18] M. Schuck and R. C. N. Pilawa-Podgurski, "Ripple minimization in asymmetric multiphase interleaved DC-DC switching converters," in *2013 IEEE Energy Conversion Congress and Exposition, ECCE 2013*, 2013, pp. 133–139, doi: 10.1109/ECCE.2013.6646691.

[19] A. A. Bakar, W. M. Utomo, T. Taufik, and A. Ponniran, "Modeling of FPGA-and DSP-based pulse width modulation for multi-input interleaved DC/DC converter," *Int. Rev. Electr. Eng.*, vol. 14, no. 1, pp. 79–85, 2019, doi: 10.15866/iree.v14i1.13928.

[20] S. Somkun, C. Sirisamphanwong, and S. Sukchai, "A DSP-based interleaved boost DC-DC converter for fuel cell applications," *Int. J. Hydrogen Energy*, vol. 40, no. 19, pp. 6391–6404, 2015, doi: 10.1016/j.ijhydene.2015.03.069.

[21] S. Shoja-Majidabad and A. Hajizadeh, "Decentralized adaptive neural network control of cascaded DC–DC converters with high voltage conversion ratio," *Appl. Soft Comput. J.*, vol. 86, p. 105878, 2020, doi: 10.1016/j.asoc.2019.105878.

[22] C. Yan, Z. Gan, and E. Salman, "Package-embedded spiral inductor characterization with application to switching buck converters," *Microelectronics J.*, vol. 66, pp. 41–47, 2017, doi: 10.1016/j.mejo.2017.05.016.

[23] E. Wang, "Current Ripple Factor of a Buck Converter," *Appl. Note*, 2014, pp. 1–5,.

[24] B. Madhaiyan, "SMPS : Non-Isolated Converters." *talemagroup*, 2020, [Online]. Availlable: https://talema.com/smps-non-isolated-converters/ .

[25] Swagtam, "Calculating Voltage, Current in a Buck Inductor," *Homemade Circuit Project*, 2019. https://www.homemade-circuits.com/calculate-current-voltage-buck-inductor/.

[26] Maxim Integrated, "Input and Output Noise in Buck Converters Explained," 2002, [Online]. Available: https://www.maximintegrated.com/en/design/technical-documents/tutorials/9/986.html.
[27] ROHM Semiconductor, "Efficiency of Buck Converter," 2016.
[28] A. Raj, "Calculating Efficiency," 2010. [Online]. Available: https://www.ti.com/lit/an/slva390a/slva390a.pdf?ts= 1648352700515&ref_url= https%253A%252F%252Fwww.google.com%252F

BIOGRAPHIES OF AUTHORS

Ahmad Faiz Hilmi Abdul Gani ⓘ 🔗 SC Ⓟ was born in Kedah, Malaysia in 1995. He received B.Eng. in Electrical Engineering from Universiti Tun Hussein Onn Malaysia (UTHM), Parit Raja, Batu Pahat, Johor, Malaysia in 2018. He is currently pursuing M.S. degree in Electrical Engineering at UTHM. His current research interests include the area of renewable energy application, multilevel DC/DC converter and soft-switching converter. He can be contacted at email: faizhilmigani@gmail.com.

Mhd Hazwaj Poad ⓘ 🔗 SC Ⓟ is a member of the IEEE and the IEEE Signal Processing Society. He has been working as a Senior Lecturer at the Department of Electronic Engineering, Faculty of Electrical and Electronic Engineering, UTHM, since 2004. He graduated from Oita University Japan, B.Eng. and M.Eng. in 2002 and 2004, respectively. His research interest is in Embedded Systems. He can be contacted at email: hazwaj@uthm.edu.my.

Afarulrazi Abu Bakar ⓘ 🔗 SC Ⓟ was born in Johor, Malaysia on May 1980. He received B.Eng. degree in Electrical Engineering from Universiti Teknologi Mara (UiTM), Malaysia, in 2004 and M.Eng and Ph.D, degrees from Universiti Tun Hussein Onn Malaysia (UTHM), in 2019 and 2007, respectively. He has been working as a Senior Lecturer at the Department of Electrical Power Engineering, Faculty of Electrical and Electronic Engineering, UTHM, since 2007. His current research interests include renewable energy application, DC/DC converters, multiple-input converters, multiphase converters, resonant converters, and advanced controller design. He can be contacted at email: afarul@uthm.edu.my.

Siti Nuraini Norazman ⓘ 🔗 SC Ⓟ was born in Johor, Malaysia on January 1996. She received B.Eng. degree in Electrical Engineering from Universiti Tun Hussein Onn Malaysia (UTHM), Parit Raja, Batu Pahat, Johor, Malaysia in 2020. She currently works as Protege at the Department of Distribution Network, LV MV Operation at Yard TNB Kempas. She can be contacted at email: sitinuraininorazman@gmail.com.

Mohd Azlee Noor Amran ⓘ 🔗 SC Ⓟ was born in Selangor, Malaysia on May 1995. He received B.Eng degree in Electrical Engineering from Universiti Tun Hussein Onn Malaysia (UTHM), Parit Raja, Batu Pahat, Johor, Malaysia in 2019. He is currently pursuing M.S. degree in Electrical Engineering at UTHM. His current research interests include the areas of DC/DC converter, system identification and controller design. He can be contacted at email: azlee013@gmail.com.